

This work has been submitted to the IEEE for possible publication. Copyright may be transferred without notice, after which this version may no longer be accessible.

arXiv:2503.04935v1 [cs.IT] 6 Mar 2025

Eliminating Phase Misalignments in Cell-Free Massive MIMO via Differential Transmission

Marx M. M. Freitas, Stefano Buzzi, *Senior Member, IEEE* and Giovanni Interdonato, *Member, IEEE*

Abstract—This paper proposes two approaches for overcoming access points’ phase misalignment effects in the downlink of cell-free massive multiple-input multiple-output (CF-mMIMO) systems. The first approach is based on the differential space-time block coding technique, while the second one is based on the use of differential modulation schemes. Both approaches are shown to perform exceptionally well and to restore system performance in CF-mMIMO systems where phase alignment at the access points for DL joint coherent transmission cannot be achieved.

Index Terms—Cell-free networks, differential space-time block coding, differential phase shift keying, phase misalignments.

I. INTRODUCTION

User-centric (UC) cell-free massive multiple-input multiple-output (CF-mMIMO) systems are a highly credited deployment for next-generation wireless networks [1]. By employing multiple access points (APs) across the coverage area to serve the user equipments (UEs), these systems can provide a more uniform spectral efficiency (SE), resistance to link blockages, and a better coverage probability than cellular networks [2].

In the downlink (DL) of CF-mMIMO systems, the APs transmitting to a specific UE need to coordinate their transmissions to ensure that their signals reach the UE antenna with perfect phase alignment, so that they can constructively add together. Achieving such alignment in practice poses significant challenges, as it demands flawless channel state information (CSI) and a shared knowledge of the phase of the local independent oscillators used at the APs for modulating information-carrying signals. Although the impact of the first factor is frequently discussed in the literature, the second, considerably more complex issue, is rarely addressed.

In this context, several approaches have emerged to assess and possibly improve the performance of CF-mMIMO systems in the presence of phase misalignment. Paper [3] proposes a rate-splitting strategy to enhance the data rate in non-coherent DL transmissions between the APs by dividing the messages into common and private parts. In [4], the energy efficiency

of coherent and non-coherent transmissions is analyzed using successive convex approximation and the Dinkelbach algorithm, and it is argued that non-coherent transmissions can serve as an alternative to coherent transmissions when fronthaul links have limited capacity. The study [5] analyzes the effects of phase misalignment within the realm of non-terrestrial networks, highlighting their significance in this environment as well. In [6], [7], a partially coherent framework is investigated. Specifically, in [6], the APs were divided into non-overlapping clusters, each managed by a dedicated central processing unit (CPU). The APs within the same cluster are assumed to be perfectly phase-aligned. Hence, the APs in the same cluster coherently transmitted the same data stream to the UE, while APs from different clusters transmitted distinct data streams. Paper [7] extends the approach in [6] by introducing an algorithm that groups APs into clusters of phase-aligned APs. Unlike [6], [7] does not rely on a very optimistic assumption of perfectly phase-aligned APs. Despite the potential of these strategies to improve the performance of CF-mMIMO systems in the presence of phase misalignment issues, none of them offered a final methodology to overcome these effects in CF-mMIMO DL transmissions. In addition, these approaches are based on the accuracy of the channel estimates, which may be ineffective in highly loaded scenarios with strong pilot contamination.

In this letter, we propose two novel approaches to mitigate the phase misalignment drawback in DL UC CF-mMIMO systems. For this purpose, the well-known differential space-time block coding (DSTBC) and differential phase-shift keying (DPSK) schemes are utilized. These techniques do not require channel knowledge at the receiver to detect the transmitted data; moreover, they are *totally immune* to phase misalignment effects during data detection, offering a promising alternative to DL coherent transmissions when APs phase misalignments are not compensated for. Numerical results will show the effectiveness of the proposed approaches, both in terms of bit-error rate (BER) and system throughput.

This letter is organized as follows. The next section contains the description of the considered system model and the mathematical model of the signal received at the UE in the presence of phase misalignments. Section III contains a brief review of DSTBC, while Section IV includes the description of the two proposed approaches to overcome APs phase misalignments in the DL. Numerical results are discussed in Section IV, while, finally, concluding remarks are provided in Section V.

II. SYSTEM MODEL

We consider a CF-mMIMO system consisting of L APs and K single-antenna UEs. The APs, each equipped with N

This work was supported by the EU under the Italian National Recovery and Resilience Plan (NRRP) of NextGenerationEU, partnership on “Telecommunications of the Future” (PE00000001 - program “RESTART”); specifically, M. M. M. Freitas was supported by Structural Project NTN, Cascade Call INFINITE, CUP D93C22000910001, while S. Buzzi and G. Interdonato were supported by Structural Project 6GWINET, Cascade Call SPARKS, CUP D43C22003080001.

The authors are with the Dept. of Electrical and Information Engineering (DIEI), University of Cassino and Southern Lazio, 03043 Cassino, Italy (e-mail: {marxmiguelmiranda.defreitas; buzzi; giovanni.interdonato}@unicas.it). S. Buzzi and G. Interdonato are also with the Consorzio Nazionale Interuniversitario per le Telecomunicazioni (CNIT), 43124 Parma, Italy. S. Buzzi is also with the Dipartimento di Elettronica, Informazione e Bioingegneria (DEIB), Politecnico di Milano, 20156 Milan, Italy.

antennas, are connected to a CPU via error-free fronthaul links. The system operates on time-division duplex (TDD) protocol and assumes reciprocity for the uplink (UL) and DL channels. We focus on DL transmissions and consider that the channel $\mathbf{h}_{k,l} \in \mathbb{C}^{N \times 1}$ between the AP l and UE k undergoes an independent correlated Rayleigh fading, being defined as¹ $\mathbf{h}_{k,l} \sim \mathcal{N}_{\mathbb{C}}(\mathbf{0}_N, \mathbf{R}_{k,l})$. Here, $\mathbf{R}_{k,l} = \mathbb{E}\{\mathbf{h}_{k,l}\mathbf{h}_{k,l}^H\} \in \mathbb{C}^{N \times N}$ represents the statistical covariance matrix of $\mathbf{h}_{k,l}$.

A. UL Training and Phase Misalignment

Each coherence block consists of τ_c complex samples, which are divided into τ_p for UL pilots and τ_d for DL data. During the UL training phase, all UEs send mutually orthogonal pilot signals to the APs for channel estimation², with some UEs reusing them if $\tau_p < K$. Once the APs receive the pilots, the channels are estimated using linear minimum mean square error (LMMSE) estimation [2].

The presence of uncompensated phase misalignments at the APs is modeled through an additional phase term that modifies the channel in an uncontrollable way. Otherwise stated, the true channel between UE k and AP l is expressed as

$$\mathbf{g}_{k,l} = e^{j\theta_l} \mathbf{h}_{k,l}, \quad (1)$$

where θ_l represents the uncontrollable phase of the oscillator in the transmit chain at the l -th AP. This phase may also include phase noise effects, and it is assumed to remain constant for at least the time required to transmit two consecutive codewords of the DSTBC, i.e., for a few symbol intervals.

B. AP Clustering and DL Transmission

In UC CF-mMIMO systems, the generic k -th UE is served by a subset of APs, called AP cluster, denoted as $\mathcal{M}_k \subset \{1, \dots, L\}$. The association policy between UEs and APs can be represented by the binary variates $a_{k,l}$, for all $k = 1, \dots, K$ and $l = 1, \dots, L$; specifically, $a_{k,l} = 1$ if $l \in \mathcal{M}_k$, and equals 0 otherwise. All the APs in \mathcal{M}_k concur to the transmission of the same data symbol to the UE k . In this letter, in order to provide a fair comparison with the DPSK scheme outlined in the following, we assume that a PSK modulation is used³. Hence, $\sum_{i=1}^K a_{i,l} \mathbf{w}_{i,l} s_i^p \in \mathbb{C}^{N \times 1}$ represents the data signal sent by AP l at discrete time epoch p . The received signal at UE k can be expressed as

$$y_k^p = \sum_{l=1}^L a_{k,l} \mathbf{g}_{k,l}^H \mathbf{w}_{k,l} s_k^p + \sum_{l=1}^L \sum_{i=1, i \neq k}^K a_{i,l} \mathbf{g}_{k,l}^H \mathbf{w}_{i,l} s_i^p + n_k^p, \quad (2)$$

where $\mathbf{w}_{i,l} \in \mathbb{C}^{N \times 1}$ denotes the precoding vector, which satisfies $\mathbb{E}\{\|\mathbf{w}_{i,l}\|^2\} = \rho_{i,l}$, with $\rho_{i,l}$ being the fraction of power allocated to the UE i regarding the AP l . The term s_i^p is the complex symbol intended for UE k at time instant p , where $p = \{1, \dots, \tau_d\}$. In addition, $n_k^p \sim \mathcal{N}_{\mathbb{C}}(0, \sigma_{\text{dl}}^2)$ denotes the receiver noise at time instant p . The detection of s_k^p given

¹The notation $\mathcal{N}_{\mathbb{C}}(\mu, \sigma^2)$ stands for a complex Gaussian random variable with mean μ and variance σ^2 , while $\mathbb{E}\{\cdot\}$ denotes statistical expectation.

²Although DSTBC does not require CSI for data detection, channel estimation is performed to compute the transmit precoders, which are crucial for suppressing co-channel interference.

³The extension of the proposed approaches to rectangular constellations will be reported in a future work.

y_k^p can be performed using the following maximum likelihood (ML) criterion

$$\hat{s}_k^p = \arg \min_{s \in \mathcal{S}} |\angle y_k^p - \angle s|^2. \quad (3)$$

where the operator $\angle \cdot$ denotes the phase.

III. A PRIMER ON DSTBC

DSTBC techniques were introduced in early '00 (see [8] for a concise yet useful treatise) for use in point-to-point MIMO systems, to enhance transmission diversity when the receiver does not have access to the CSI. They represent the differential version of classical space-time codes that permit achieving diversity gain by leveraging the use of multiple antennas at the transmitter and (possibly) at the receiver. In the following, we briefly review useful concepts related to DSTBC.

Let us consider a system with N_t antennas at the transmitter and one antenna at the receiver, and let P represent the number of symbol periods spanned by a space-time codeword. Let $\mathcal{S} = \{s^1, s^2, \dots, s^J\}$ denote the set of J complex symbols, drawn from a unitary constellation, to be transmitted to the receiver in a given channel realization. Then, \mathcal{S} is divided into smaller subsets, each containing n_s symbols. Let us denote by $\mathcal{S}^t = \{s^{(t-1)n_s+1}, \dots, s^{tn_s}\}$ the t -th subset of \mathcal{S} , and by $G = \lfloor \tau_d/P \rfloor$, where $\lfloor \cdot \rfloor$ is the floor operation, their number.

Each subset \mathcal{S}^t is then mapped onto a code matrix $\mathbf{X}^t \in \mathbb{C}^{N_t \times P}$, with t also serving as the index of the code matrix. For the DL data decoding procedure to be feasible, \mathbf{X}^t must be a unitary matrix, i.e., it has to satisfy the condition $(\mathbf{X}^t)^H \mathbf{X}^t = \mathbf{I}_{N_t}$. Another desirable property is orthogonality, which helps reduce the computational complexity of detection at the receiver. However, orthogonal STBC matrices exhibit only a semi-unitary structure. Specifically, they satisfy the relation $(\mathbf{X}^t)^H \mathbf{X}^t = \sum_{j=1}^{n_s} |s^j|^2 \mathbf{I}_{N_t}$. To make \mathbf{X}^t unitary, \mathbf{X}^t is typically multiplied by a factor of $1/\sqrt{n_s}$.

A widely known orthogonal code matrix in the literature is the Alamouti matrix, which encodes two symbols ($n_s = 2$) across two transmit antennas ($N_t = 2$) and two symbol periods ($P = 2$). The Alamouti matrix is expressed as

$$\mathbf{X}^t = \frac{1}{\sqrt{2}} \begin{bmatrix} s^1 & (s^2)^* \\ s^2 & -(s^1)^* \end{bmatrix}, \quad (4)$$

where s^1 and s^2 are symbols taken from a generic subset \mathcal{S}^t . For configurations with more transmit antennas, other orthogonal matrices exist; as an example, if $N_t = 4$, the following orthogonal code matrix can be employed

$$\mathbf{X}^t = \frac{1}{\sqrt{3}} \begin{bmatrix} s^1 & 0 & s^2 & -(s^3)^* \\ 0 & s^1 & (s^3)^* & (s^2)^* \\ -(s^2)^* & -(s^3)^* & (s^1)^* & 0 \\ (s^3)^* & -(s^2)^* & 0 & (s^1)^* \end{bmatrix}. \quad (5)$$

This code matrix sends $n_s = 3$ symbols over $P = 4$ symbol periods, thus having the code rate of $R = 3/4$.

Once the data symbols are mapped onto \mathbf{X}^t for $t = \{1, \dots, G\}$, \mathbf{X}^t is differentially encoded by forming a new matrix

$$\mathbf{C}^t = \mathbf{C}^{t-1} \mathbf{X}^t, \quad (6)$$

where $\mathbf{C}^0 = \mathbf{I}_{N_t}$. Since \mathbf{X}^t is unitary, it readily follows that $(\mathbf{C}^t)^H \mathbf{C}^t = \mathbf{I}_{N_t}$. If \mathbf{C}^t is transmitted to a single-antenna UE

over P consecutive time intervals, the received block signal can be expressed as the following P -dimensional row vector:

$$\mathbf{y}^t = \mathbf{h}^H \mathbf{C}^{t-1} \mathbf{X}^t + \mathbf{n}^t, \quad (7)$$

with $\mathbf{n}^t \sim \mathcal{N}_{\mathbb{C}}(\mathbf{0}, \sigma_{\text{dl}}^2 \mathbf{I}_{N_t})$ representing the receiver noise and $\mathbf{h}^H \mathbf{C}^{t-1}$ denoting the term that is unknown at the receiver. Then, \mathbf{X}^t can be decoded by using two consecutive received blocks, i.e., \mathbf{y}^t and \mathbf{y}^{t-1} , where $\mathbf{y}^{t-1} = \mathbf{h}^H \mathbf{C}^{t-1} + \mathbf{n}^{t-1}$. The ML detection of \mathbf{X}^t corresponds to compute $\hat{\mathbf{X}}^t = \arg \min_{\mathbf{X} \in \mathcal{X}_N} \|\mathbf{y}^t(\mathbf{X})^H - \mathbf{y}^{t-1}\|^2$ or equivalently [8]

$$\hat{\mathbf{X}}^t = \arg \max_{\mathbf{X} \in \mathcal{X}_N} \text{ML}^t, \quad (8)$$

where \mathcal{X}_N denotes the set of all possible code matrices for a given unitary constellation \mathcal{S} . The term ML^t is obtained as

$$\text{ML}^t = \text{tr} \left\{ \text{Re} \left\{ \mathbf{X} (\mathbf{y}^t)^H \mathbf{y}^{t-1} \right\} \right\}. \quad (9)$$

IV. DL TRANSMISSION SCHEMES ROBUST TO PHASE MISALIGNMENT

This section presents the proposed approaches to mitigate phase misalignment effects in UC CF-mMIMO systems based on DSTBC and DPSK schemes. Specifically, it demonstrates how to adapt them to the CF-mMIMO scenario.

A. Differential STBC for CF-mMIMO Systems

To perform differential STBC techniques in CF-mMIMO, we proceed as follows. First of all, a specific DSTBC scheme is chosen, e.g., (4) or (5), even though many more choices are available [8]. Next, each UE must be connected to a number of APs equal to the number of rows of the selected DSTBC matrix. Then, with reference to UE k , the CPU encodes \mathbf{X}_k^t differentially as in (6). That is, it generates the information signal $\mathbf{C}_k^t \in \mathbb{C}^{L_k \times L_k}$ to be transmitted to the UE k . Since the transmission involves multiple APs instead of multiple antennas on a single transmitter, the CPU then splits \mathbf{C}_k^t among the APs serving the UE k , as depicted in Fig. 1. Specifically, each row of the information matrix \mathbf{C}_k^t will be assigned to one of the APs serving UE k ; the elements of the rows of \mathbf{C}_k^t will be transmitted by the associated APs over P consecutive time intervals. It is thus evident that in our proposed approach, each AP acts like a single antenna of the original DSTBC, and the multiple antennas at the AP are used to suppress multi-user interference, not to perform the differential space-time coding task. The row of \mathbf{C}_k^t that the CPU assigns to AP l is computed as

$$\mathbf{c}_{k,l}^t = [\mathbf{C}_k^{t-1}]_{m(l,k),:} \mathbf{X}_k^t, \quad (10)$$

where $l \in \mathcal{M}_k$ and $m(l,k) \in \{1, \dots, L_k\}$ is a mapping function that points to the row of matrix \mathbf{C}_k^t to be sent to AP l for transmission to UE k . Let $\sum_{k=1}^K a_{k,l} \mathbf{w}_{k,l} \mathbf{c}_{k,l}^t \in \mathbb{C}^{N \times L_k}$ represent the signal sent by AP l . The received signal block at UE k can be expressed as

$$\mathbf{y}_k^t = \sum_{l=1}^L g_{k,l}^{(\text{ef})} [\mathbf{C}_k^{t-1}]_{m(l,k),:} \mathbf{X}_k^t + \tilde{\mathbf{n}}_k^t, \quad (11)$$

with $g_{k,l}^{(\text{ef})} = a_{k,l} \mathbf{g}_{k,l}^H \mathbf{w}_{k,l} \in \mathbb{C}$ representing the *effective* DL channel of UE k . Moreover,

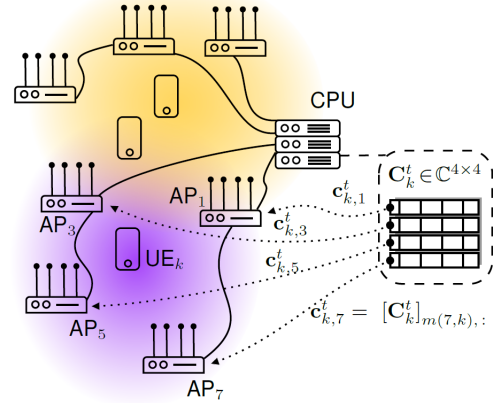


Fig. 1: An illustration of how the information signal \mathbf{C}_k^t , designed at the CPU, is row-wise split among the APs serving UE k . Each row of matrix \mathbf{C}_k^t is assigned to the corresponding AP according to the mapping function $m(\cdot, k)$. In this example, the APs transmit the elements of the assigned row over $L_k = 4$ consecutive symbol intervals. As an example of the meaning of the mapping $m(l, k)$, note that, since the fourth row of the matrix \mathbf{C}_k^t is sent to AP7, we have that $m(7, k) = 4$.

$$\tilde{\mathbf{n}}_k^t = \sum_{i=1, i \neq k}^K \sum_{l=1}^L \tilde{g}_{i,k,l}^{(\text{ef})} [\mathbf{C}_i^{t-1}]_{m(l,i),:} \mathbf{X}_i^t + \mathbf{n}_k^t \quad (12)$$

stands for the combined effects of interference and receiver noise, where $\tilde{g}_{i,k,l}^{(\text{ef})} = a_{i,l} \mathbf{g}_{k,l}^H \mathbf{w}_{i,l}$. One can note that (11) resembles (7), as both assume that CSI is not available at the receiver. Nevertheless, (11) provides a more general expression, as it is computed based on $g_{k,l}^{(\text{ef})}$, which incorporates the effects of $\mathbf{h}_{k,l}$, the precoding, and phase misalignment.

To detect the code matrix \mathbf{X}_k^t , the UE k utilizes the ML criterion defined in (8). However, the computation of ML_k^t in (9) is based on the received signal model defined in (11). To solve ML_k^t , \mathbf{y}_k^{t-1} is given by $\mathbf{y}_k^{t-1} = \sum_{l=1}^L g_{k,l}^{(\text{ef})} [\mathbf{C}_k^{t-1}]_{m(l,k),:} + \tilde{\mathbf{n}}_k^{t-1}$, where $\tilde{\mathbf{n}}_k^{t-1}$ is computed as $\tilde{\mathbf{n}}_k^{t-1} = \sum_{i=1, i \neq k}^K \sum_{l=1}^L \tilde{g}_{i,k,l}^{(\text{ef})} [\mathbf{C}_i^{t-1}]_{m(l,i),:} + \mathbf{n}_k^{t-1}$. Using the decision rule (9), the effects of phase misalignment are removed from the desired signal components of UE k , as shown in the appendix.

B. DPSK for CF-mMIMO

DL coherent transmissions based on DPSK schemes lie as a middle ground between conventional CF-mMIMO systems and the above outlined DSTBC schemes. That is, the information signal is transmitted individually at each time discrete time epoch p , for $p = 1, \dots, \tau_d - 1$, and the received signal model follows (2). However, the data symbols are differentially encoded. Let $\sum_{i=1}^K a_{i,l} \mathbf{w}_{i,l} \mathbf{c}_{i,l}^p \in \mathbb{C}^{N \times L_k}$ denote the signal transmitted by AP l . The received signal at UE k can be modeled as

$$\mathbf{y}_k^p = \sum_{l=1}^L a_{k,l} \mathbf{g}_{k,l}^H \mathbf{w}_{k,l} \mathbf{c}_k^p + \sum_{l=1}^L \sum_{i=1, i \neq k}^K a_{i,l} \mathbf{g}_{k,l}^H \mathbf{w}_{i,l} \mathbf{c}_i^p + \mathbf{n}_k^p, \quad (13)$$

where \mathbf{c}_k^p is calculated as $\mathbf{c}_k^p = \mathbf{c}_k^{p-1} s_k^p$, and $\mathbf{c}^{p-1} \in \mathbb{C}$ denotes the information signal transmitted at the previous time instant, with $\mathbf{c}_k^0 = 1$. Furthermore, since s_k^p is taken from a unitary constellation, $(\mathbf{c}_k^{p-1})^H \mathbf{c}_k^{p-1} = 1$. The ML detection of s_k^p given

y_k^p and y_k^{p-1} can be computed as [8]:

$$\hat{s}_k^p = \arg \max_{s \in \mathcal{S}} \left\{ \text{Re} \left\{ s (y_k^p)^* y_k^{p-1} \right\} \right\}. \quad (14)$$

Pros and Cons of the Proposed Approaches: The suggested methods enable DL data decoding without requiring CSI at the receiver. Specifically, CSI estimates are utilized solely at the network side to calculate precoding vectors for the APs. These approaches help mitigate phase misalignment in DL transmissions. They are adaptable and compatible with any AP selection strategy, with the only requirement being that each UE must be served by a number of APs matching the row count of the chosen DSTBC matrix. Conversely, it's important to note that with the DPSK strategy, the modulation is restricted to PSK, while in DSTBC, the network's performance might be constrained by the code matrix rate⁴, expressed as the ratio $R = n_s/P$. For example, for $N_t > 4$, the code rates can significantly drop from $R = 3/4$. The Alamouti matrix shown in (4) is a particular instance with a code rate of 1 [8]. Lastly, data detection in DSTBC demands more computation than in DPSK, though, in the case of the here considered DSTBC, decisions on data symbols can be made independently, vastly simplifying the decision rule (8).

V. NUMERICAL RESULTS

Unless stated otherwise, we consider a CF-mMIMO network consisting of $K = 20$ single-antenna UEs and $L = 40$ APs, each equipped with $N = 4$ antennas. Moreover, each UE is served by $L_k = 4$ APs. The K UEs are uniformly distributed over a square area of 0.5×0.5 km, while the positions of the APs follow a hard core point process (HCPP)⁵. The simulations focus on DL channels, with the following parameters: $\tau_c = 200$, $\tau_p = 10$, and $\tau_d = 190$. The total transmission powers per UE and AP are set to 100 mW and 200 mW. To compute the oscillator phases θ_l , we utilize the discrete-time Wiener phase model [9].

To calculate the BER and SE, we perform Monte-Carlo simulations to account for different channel realizations and AP/UE locations, referred to as setups. For each setup, the received symbols (detected using the ML criterion) are mapped to bits using the Gray code, and the BER is computed for each UE over all channel realizations. The SE for UE k in each setup is computed as:

$$\text{SE}_k = P_f \log_2 (M_o) (1 - \mathbb{E} \{ \text{BER}_k \}) \quad (15)$$

where M_o is the modulation order and $\mathbb{E} \{ \text{BER}_k \}$ is average BER across all channel realizations. It is assumed that the modulation order is $M_o = 8$. Moreover, P_f is the pre-log factor, representing the fraction of samples in each coherence block dedicated to DL data transmissions. P_f is given by τ_d/τ_c for conventional CF-mMIMO, $(\tau_d - 1)/\tau_c$ for CF-mMIMO with DPSK, and $(G - 1)n_s/\tau_c$ for CF-mMIMO. The AP

⁴SE results shown in the next section will permit evaluating the impact of the DSTBC rate.

⁵This method ensures a minimum distance of $d_{\min} = \sqrt{A/L}$ between any two APs, where A is the coverage area. Initially, the APs are placed using a homogeneous Poisson point process with a mean rate of $1/d_{\min}$. Then, the locations of any APs that do not meet the spacing requirement are randomly updated until the condition is satisfied.

TABLE I: SIMULATION SETTINGS

Parameter	Value
Shadow fading standard deviation, σ_{SF}	4 dB
AP/UE antenna height, $h_{\text{AP}}, h_{\text{UE}}$	11.65 m, 1.65 m
RX noise figure (NF)	8 dB
Carrier frequency, bandwidth	3.5GHz, 20MHz
Angular standard deviations (ASDs)	$\sigma_\varphi = \sigma_\theta = 15^\circ$
Antenna spacing	1/2 wavelength distance

clustering scheme that jointly performs the pilot assignment and AP selection is utilized [2]. In this scheme, each UE is first associated with a coordination AP. Then, the APs serve only the UEs with the strongest channel gain in each pilot. The first τ_p UEs are assigned to orthogonal pilots, while the remaining ones are assigned to the pilot that causes the least contamination in each AP. In the following, it is assumed that each UE will be connected to the N_t APs with the strongest channel gains within its AP cluster (or in its surroundings if $L_k < N_t$), subject to the constraint that no AP is connected to more than τ_p UEs. We consider two types of processing: centralized and distributed. In the centralized one, the network processing (e.g., channel estimation and precoding vector generation) is centralized at the CPU. In the distributed one, the processing is distributed among the APs.

The power coefficients at AP l in the distributed processing are given by $\rho_{k,l} = \rho_d \sqrt{\beta_{k,l} / \sum_{k' \in \mathcal{D}_l} \beta_{k',l}}$, where ρ_d is the maximum DL transmit power per AP. For the centralized one, the fractional power control is utilized [2]. To compute the precoding vectors, the partial MMSE (P-MMSE) and local partial MMSE (LP-MMSE) are used for centralized and distributed processing, respectively [2]. The 3GPP Urban Micro (UMi) path loss model is adopted for modeling the propagation channel [10]. It is considered that the shadowing terms of an AP to different UEs are correlated, and the computation of correlation matrices $\mathbf{R}_{k,l}$ follows the local scattering spatial correlation model [2]. Table I exhibits the parameters used in the models [2], [11].

Fig. 2 presents the CDFs of the average BER and SE for CF-mMIMO systems with (Async CF) and without phase misalignment (Sync CF). Both are compared with the proposed approaches. One can note that phase misalignment degrades the BER of CF-mMIMO systems performing DL coherent transmission. However, this degradation can be mitigated by employing differential schemes, such as DSTBC and DPSK. This improvement is due to the ability of differential schemes to mitigate phase misalignment effects. Among these, CF-mMIMO systems using DSTBC achieve a lower BER than those employing DPSK, as DSTBC not only mitigates phase misalignment, but also optimally enhances transmission diversity.

On the other hand, the SE of DSTBC is not as high as that of the DPSK scheme. This difference is due to the pre-log factor of DSTBC schemes, which is influenced by the code rate R , which is $R = 3/4$ for $L_k = N_t = 4$. Nonetheless, the code rate does not limit DSTBC schemes for $L_k = 2$, since $R = 1$, as depicted in Fig. 3. Moreover, the performance gap between CF-mMIMO systems without phase misalignment and those employing differential schemes can be reduced if the APs are equipped with more antennas, such as $N = 10$.

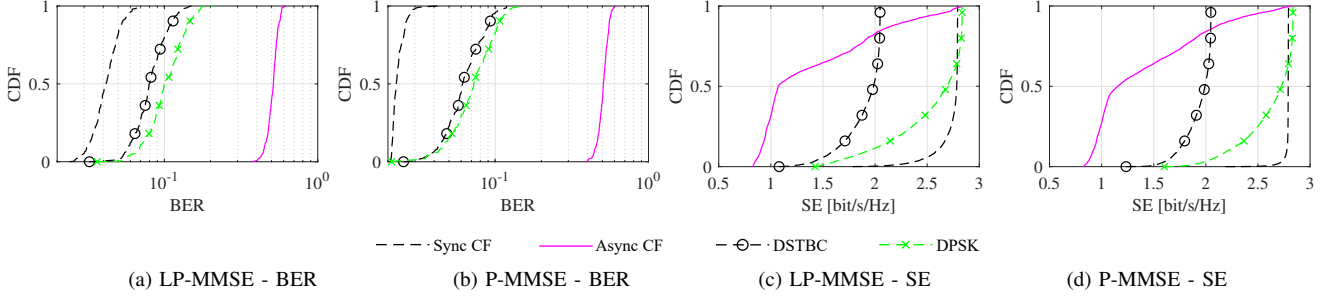


Fig. 2: Cumulative distribution function (CDF) of the average BER and SE for each setup. Parameters setting: $L = 40$, $K = 20$, $N = 4$, and $L_k = 4$.

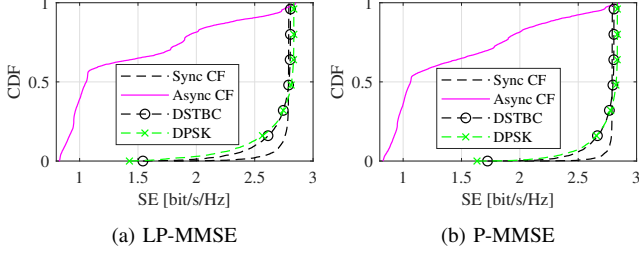


Fig. 3: CDF of the SE for the proposed approaches and synchronized CF-mMIMO system. Here, $L=40$, $K=20$, $N=10$, and $L_k=2$.

Finally, although not shown in this paper due to space constraints, our results confirm that the previous conclusions hold as the number of UEs K increases. That is, differential schemes continue to mitigate phase misalignment effects. However, the SE of DSTBC degrades slightly more as K increases. For instance, the SE of the DSTBC decreases by about 16.9% for the 95% likely UEs when K increases from 20 to 40, while the SE of DPSK decreases by about 15% for the P-MMSE scheme. These results show that the DPSK technique was slightly more resilient to interference effects than DSTBC strategies in the considered scenario.

VI. CONCLUSIONS

This paper proposed two novel approaches to mitigate phase misalignment effects in UC CF-mMIMO systems performing coherent DL transmission. The first approach is based on the DSTBC scheme, while the second relies on DPSK. We demonstrated how to adapt these techniques to a CF-mMIMO scenario and provided a mathematical proof of how DSTBC overcomes phase misalignment in CF-mMIMO systems. The proposed approaches were compared to a conventional UC CF-mMIMO network performing DL coherent transmission. The simulation results revealed that the BER and SE of conventional CF-mMIMO systems are severely degraded by phase misalignment, and that the proposed differential schemes are exceptionally effective in restoring performance.

APPENDIX A

PROOF OF PHASE MISALIGNMENT MITIGATION

We now show how phase misalignment effects can be mitigated in a CF-mMIMO system using DSTBC for DL transmission, based on the received signal model in (11). By letting $\mathbf{DS}_k^t = \sum_{l=1}^L g_{k,l}^{(\text{ef})} [\mathbf{C}_k^{t-1}]_{m(l,k),:}$, \mathbf{X}_k^t denote the desired signal of UE k , (9) can be rewritten as

$$\text{ML}_k^t = \text{Re} \{ \text{tr} \{ \mathbf{X}_k (\mathbf{Y}_{k,1} + \mathbf{Y}_{k,2} + \mathbf{Y}_{k,3} + \mathbf{Y}_{k,4}) \} \}, \quad (16)$$

with $\mathbf{Y}_{k,1} = (\mathbf{DS}_k^t)^H \mathbf{DS}_k^{t-1}$ denoting the desired signal components and the remaining terms corresponding to cross-products, calculated as $\mathbf{Y}_{k,2} = (\mathbf{DS}_k^t)^H \tilde{\mathbf{n}}_k^{t-1}$, $\mathbf{Y}_{k,3} = (\tilde{\mathbf{n}}_k^t)^H \mathbf{DS}_k^{t-1}$, and $\mathbf{Y}_{k,4} = (\tilde{\mathbf{n}}_k^t)^H \tilde{\mathbf{n}}_k^{t-1}$. Assuming that \mathbf{X}_k^t is detected and since $\mathbf{X}_k^t (\mathbf{X}_k^t)^H = \mathbf{I}_{L_k}$, the product $\mathbf{X}_k^t \mathbf{Y}_{k,1}$ in (16) is calculated as

$$\sum_{l=1}^L \sum_{l'=1}^L g_{k,l}^{(\text{ef})H} g_{k,l'}^{(\text{ef})} \left([\mathbf{C}_k^{t-1}]_{m(l,k),:} \right)^H [\mathbf{C}_k^{t-1}]_{m'(l',i),:}. \quad (17)$$

Since the data symbols are taken from a unitary constellation, i.e., $|s| = 1$ for all $s \in \mathcal{S}$, the code matrices considered in this paper satisfy the property $\text{tr} \{ ([\mathbf{C}_k^{t-1}]_{m(l,k),:})^H [\mathbf{C}_k^{t-1}]_{m(l,k),:} \} = 1$. Moreover, $\text{tr} \{ ([\mathbf{C}_k^{t-1}]_{m(l,k),:})^H [\mathbf{C}_k^{t-1}]_{m'(l',i),:} \} = 0$ for $m' \neq m$ and $l \neq l'$. Consequently, $\text{tr} \{ \mathbf{X}_k^t \mathbf{Y}_{k,1} \}$ is obtained as

$$\text{tr} \{ \mathbf{X}_k^t \mathbf{Y}_{k,1} \} = \sum_{l=1}^L g_{k,l}^{(\text{ef})H} g_{k,l}^{(\text{ef})} = \sum_{l=1}^L |g_{k,l}^{(\text{ef})}|^2. \quad (18)$$

Therefore, although the interfering components (cross products) remain affected by phase misalignment, their impact on the desired signal is mitigated by the product $g_{k,l}^{(\text{ef})H} g_{k,l}^{(\text{ef})}$.

REFERENCES

- [1] H. Q. Ngo, G. Interdonato, E. G. Larsson, G. Caire, and J. G. Andrews, "Ultradense cell-free massive MIMO for 6G: Technical overview and open questions," *Proc. of the IEEE*, vol. 112, no. 7, pp. 805–831, 2024.
- [2] Ö. Demir *et al.*, *Foundations of User-Centric Cell-Free Massive MIMO*. Foundations and Trends® in Signal Processing, 2021, vol. 14, no. 3-4.
- [3] J. Zheng, J. Zhang, J. Cheng, V. C. M. Leung, D. W. K. Ng, and B. Ai, "Asynchronous cell-free massive MIMO with rate-splitting," *IEEE J. Sel. Areas Commun.*, vol. 41, no. 5, pp. 1366–1382, 2023.
- [4] R. P. Antonioli *et al.*, "On the energy efficiency of cell-free systems with limited fronthauls: Is coherent transmission always the best alternative?" *IEEE Trans. Wireless Commun.*, vol. 21, no. 10, pp. 8729–8743, 2022.
- [5] C. D'Andrea *et al.*, "Coherent vs. non-coherent joint transmission in cell-free user-centric non-terrestrial wireless networks," in *Proc. IEEE Int. Workshop Signal Process. Advances in Wireless Commun. (SPAWC)*, 2024, pp. 636–640.
- [6] R. P. Antonioli, I. M. Braga, G. Fodor, Y. C. Silva, and W. C. Freitas, "Mixed coherent and non-coherent transmission for multi-CPU cell-free systems," in *Proc. IEEE Int. Conf. Commun.*, 2023, pp. 1068–1073.
- [7] K. Ganesan *et al.*, "Cell-free massive MIMO with multi-antenna users and phase misalignments: A novel partially coherent transmission framework," *IEEE Open J. Commun. Soc.*, vol. 5, pp. 1639–1655, 2024.
- [8] E. G. Larsson and P. Stoica, "Space-time block coding for wireless communications," *Cambridge University Press*, 2003.
- [9] E. Björnson, M. Matthaiou, and M. Debbah, "Massive MIMO with non-ideal arbitrary arrays: Hardware scaling laws and circuit-aware design," *IEEE Trans. Wireless Commun.*, vol. 14, no. 8, pp. 4353–4368, 2015.
- [10] 3GPP, *Study on channel model for frequencies from 0.5 to 100 GHz*, 2019, 3GPP TR 38.901 (Release 16).
- [11] 3GPP, *NR; User Equipment (UE) radio transmission and reception; Part 1: Range 1 Standalone*, 2021, 3GPP TR 38.101-1 (Release 17).